



Limits on Violations of Lorentz Symmetry and the Einstein Equivalence Principle using Radio-Frequency Spectroscopy of Atomic Dysprosium

M. A. Hohensee,* N. Leefer, and D. Budker

Physics Department, University of California, Berkeley 94720, USA

C. Harabati, V. A. Dzuba, and V. V. Flambaum

School of Physics, University of New South Wales, Sydney 2052, Australia

(Received 14 March 2013; published 29 July 2013)

We report a joint test of local Lorentz invariance and the Einstein equivalence principle for electrons, using long-term measurements of the transition frequency between two nearly degenerate states of atomic dysprosium. We present many-body calculations which demonstrate that the energy splitting of these states is particularly sensitive to violations of both special and general relativity. We limit Lorentz violation for electrons at the level of 10^{-17} , matching or improving the best laboratory and astrophysical limits by up to a factor of 10, and improve bounds on gravitational redshift anomalies for electrons by 2 orders of magnitude, to 10^{-8} . With some enhancements, our experiment may be sensitive to Lorentz violation at the level of 9×10^{-20} .

DOI: [10.1103/PhysRevLett.111.050401](https://doi.org/10.1103/PhysRevLett.111.050401)

PACS numbers: 03.30.+p, 04.80.-y, 11.30.Cp, 32.30.Jc

Local Lorentz invariance (LLI) and the Einstein equivalence principle (EEP) are fundamental to both the standard model and general relativity [1]. Nevertheless, these symmetries may be violated at experimentally accessible energy scales due to spontaneous symmetry breaking, or some other mechanism at high energy scales [2,3]. This has motivated the development of many experimental tests of both LLI and EEP [4,5], and of a phenomenological framework, known as the standard model extension (SME), which can be used to quantitatively compare these tests' results to one another [6]. This widely used [4] framework augments the standard model Lagrangian with every combination of standard model fields that are not term-by-term invariant under Lorentz transformations, while maintaining gauge invariance, energy-momentum conservation, and Lorentz invariance of the total action [6]. Violations of LLI, which themselves constitute violations of EEP [1,5], have also been shown to violate other tenets of general relativity [7].

In this Letter, we show, using many-body calculations, that the energies of two low-lying excited states of dysprosium (Dy) [8–11] are extremely sensitive to physics that breaks LLI and the EEP in the dynamics of electrons. We report the results of an analysis of Dy spectroscopy data acquired over two years that significantly improves upon the best laboratory [12] and accelerator [13] limits on electron violations of LLI and EEP. Our result is competitive with some astrophysical bounds [14]. We also improve constraints on electron-related gravitational redshift anomalies [15] by 2 orders of magnitude [16].

The EEP and LLI require that spacetime, while it may be curved, be locally flat, and Lorentzian [1]. Thus, the relative frequencies of any set of clocks at relative rest and located at the same point in (or within a sufficiently small

volume of) spacetime must be independent of (a) where that point is located in a gravitational potential, and (b) the velocity and orientation of their rest frame (LLI). In the SME, violation of EEP and LLI for electrons can be described by modifying the electron dispersion relation, which in turn causes the energies of bound electronic states to vary with the velocity, orientation, and gravitational potential of their rest frame [7,17].

We focus on the symmetric, traceless $c_{\mu\nu}$ tensor in the electron sector of the SME, written using coordinates such that the speed of light is a constant c in all frames. The $c_{\mu\nu}$ tensor modifies the kinetic term in the electronic QED Lagrangian to become [6]

$$\mathcal{L} = \frac{1}{2} i \bar{\psi} (\gamma_\nu + c_{\mu\nu} \gamma^\mu) \bar{D}^\nu \psi - \bar{\psi} m \psi, \quad (1)$$

where m is the electron mass, ψ is a four-component Dirac spinor, γ^ν are the Dirac gamma matrixes, and $f \bar{D}^\nu g \equiv f D^\nu g - g D^\nu f$, with $D^\nu \equiv \partial^\nu - iqA^\nu$. The $c_{\mu\nu}$ tensor is frame dependent [6,17–19], and is uniquely specified by its value in a standard reference frame. We use the Sun-centered, celestial equatorial frame (SCCEF) for this purpose, indicated by the coordinate indexes (T, X, Y, Z), for ease of comparison with other results [4]. The component indexes for laboratory frame coordinates are given as (0, 1, 2, 3), where $t = x_0/c$ is the time coordinate. Roman indexes are used to indicate the spatial components of $c_{\mu\nu}$, and are capitalized in the SCCEF frame. The $c_{\mu\nu}$ tensor has six parity-even components: c_{TT} , plus the five c_{JK} 's; and three parity-odd components: c_{TJ} , which introduce direction and frame dependent anisotropies in the electrons' energy momentum, or dispersion relation [6]. This shifts the energies of bound electronic states as a function of the states' orientation and alignment in absolute space,

breaking both LLI and rotational symmetry [17]. In a gravitational potential, Eq. (1) acquires additional terms proportional to $c_{\mu\nu}$ and to the curvature of spacetime [7]. These arise due to the interplay between the LLI-preserving distortion of spacetime due to gravity, and the LLI-violating distortion due to $c_{\mu\nu}$, generating anomalous gravitational redshifts that scale with the electron's kinetic energy [7,16].

In terms of spherical-tensor operators, Eq. (1) produces a shift δh in the effective Hamiltonian for a bound electron with momentum \vec{p} given by [7,17,20]

$$\delta h = -\left(C_0^{(0)} - \frac{2U}{3c^2}c_{00}\right)\frac{\vec{p}^2}{2m} - \sum_{q=-2}^2 \frac{(-1)^q}{6m} C_q^{(2)} T_{-q}^{(2)}, \quad (2)$$

where we have included the leading order $(2U/3c^2)c_{00}$ gravitational redshift anomaly [7,21] in terms of the Newtonian potential U , and

$$\begin{aligned} C_0^{(0)} &= c_{00} + (2/3)c_{jj}, \\ C_0^{(2)} &= (c_{jj} - 3c_{33}) \\ C_{\pm 1}^{(2)} &= \pm 6(c_{31} \pm ic_{32}), \\ C_{\pm 2}^{(2)} &= 3(c_{11} - c_{22} \pm 2ic_{12}), \end{aligned}$$

are written in terms of the laboratory-frame values of the $c_{\mu\nu}$ tensor, with summation implied over like indexes. Note that $C_0^{(2)}$ is also known as c_q in the literature [17]. The spherical tensor components of the squared momentum are written as $T_0^{(2)} = \vec{p}^2 - 3p_3^2$, $T_{\pm 1}^{(2)} = \pm p_3(p_1 \pm ip_2)$, and $T_{\pm 2}^{(2)} = (p_1^2 - p_2^2)/2 \pm ip_1p_2$. The energy shift for a state $|J, M\rangle$ of an atom due to the perturbation (2) is the expectation value of the corresponding N electron operator. Since only tensors with $q = 0$ contribute to energy shifts of bound states, we need only calculate matrix elements for the \vec{p}^2 and $T_0^{(2)} = \vec{p}^2 - 3p_3^2$ operators.

Dysprosium, an atom with 66 protons and a partially filled f -shell, is well suited to measuring the electron $c_{\mu\nu}$ coefficients. It possesses two near-degenerate, low-lying excited states with significant momentum quadrupole moments, opposite parity, and leading configurations: $[\text{Xe}]4f^{10}5d6s$, $J = 10$ (state A) and $[\text{Xe}]4f^95d^26s$, $J = 10$ (state B), which differ by a transposition of an electron from the $4f$ to the $5d$ orbital. The energy difference between these states can be measured directly by driving an electric-dipole transition (Fig. 1) with a radio-frequency (rf) field, and should be particularly sensitive to anomalies proportional to the electrons' kinetic energy, since the $4f$ orbital lies partly within the radius of filled s , p , and d shells that screen the nuclear charge from the larger $5d$ orbital.

To calculate the relevant matrix elements for these states, we use a version of the configuration interaction method optimized for atoms with many electrons in open shells. This method has been used to calculate energy

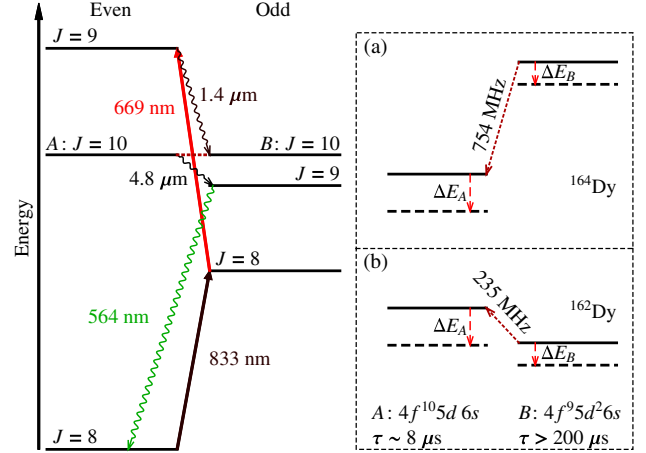


FIG. 1 (color online). Energy levels of Dysprosium. Atoms are optically pumped (solid lines) to a state which decays (wavy lines) into the metastable state B. A linearly polarized rf field drives the $B \rightarrow A$ transition, which is detected via fluorescence at 564 nm. Insets (a) and (b) show the magnified diagram for ^{164}Dy and ^{162}Dy , respectively. Lorentz-symmetry violation shifts the rf resonance by $\delta\omega_{\text{rf}} = (\Delta E_B - \Delta E_A)/\hbar$. The sign of the observed shift depends on the sign of the level splitting.

levels, transition amplitudes, dynamic polarizabilities, “magic” frequencies in optical traps, and the effects of α variation and parity violation in Dy and other atoms [22,23]. Calculated values of the reduced matrix elements for the A and B states of Dy are presented in Table I, and details of their derivation can be found in the Supplemental Material [26]. To check our results, we calculate the fully relativistic matrix elements of $c\gamma^0\gamma^j p_j$ and $T_0^{(2)} = c\gamma^0(\gamma^j p_j - 3\gamma^3 p_3)$, corresponding to \vec{p}^2 and $\vec{p}^2 - 3p_3^2$ [20]. We find good agreement between both calculations, consistent with our initial approximation and intuition. Measurements of the Dy $B \rightarrow A$ transition are highly sensitive to violations of LLI and EEP because the electrons have more kinetic energy in state A than they do in state B. The same transition is particularly useful for probing variations in the fine structure constant α , where it is the

TABLE I. Matrix elements of the relevant operators of Lorentz violation for the states A and B of Dy in units of the Hartree energy $E_h = (6.5 \times 10^{15} \text{ Hz})\hbar$.

| | State A | State B |
|---|----------------------------------|----------------|
| Term symbol | $^3[10]$ | $^7\text{H}^o$ |
| | Energies (cm^{-1}) | |
| Experiment [24] | 19798 | 19798 |
| Calculation [25] | 19786 | 19770 |
| | Matrix element (units of E_h) | |
| $\langle J \ c\gamma^0(\gamma^j p_j - 3\gamma^3 p_3) \ J \rangle$ | 69.48 | 49.73 |
| $\langle J \ \vec{p}^2 - 3p_3^2 \ J \rangle$ | 69.84 | 49.89 |
| $\langle JM \vec{p}^2 JM \rangle$ | 437 | 422 |

energy of state B that depends most strongly on the value of α [11,27–29].

An effusive atomic beam of Dysprosium atoms is produced by a ~ 1400 K oven, and is optically pumped into the metastable state B via consecutive laser excitations with 833 and 669 nm light, followed by a spontaneous decay. The atoms are resonantly excited from state B to A via an rf electric field, whose linear polarization defines the atoms' quantization axis. The polarization of the excitation laser is chosen to create a symmetric population among the $\pm M$ magnetic sublevels of state B to suppress the effects of Zeeman shifts on our measurement. Magnetic shielding and Helmholtz coils allow us to cancel background magnetic fields at the level of 20 μG . The A state relaxes to the ground state in a cascade decay, emitting 564 nm light in the process. The transition frequency is determined by measuring the intensity of the 564 nm fluorescence (with a photomultiplier) as a function of radio frequency, defined relative to a HP5061A Cs frequency reference. The fractional frequency stability of this reference is rated at better than 10^{-12} for 10^4 s of averaging. We continuously compare the Cs reference to a GPS disciplined Symmetricom TS2700 Rb oscillator, to verify that the fractional drift of the reference is less than 10^{-11} over the entire period that data were collected. Our results depend upon rf measurements with fractional precision larger than 10^{-10} , and thus we neglect instabilities in the frequency reference in what follows. More details regarding the experimental procedure and apparatus can be found in Refs. [28,30].

We measure the average frequency shift of all populated magnetic sublevels of state B relative to those of state A that are coupled by the rf electric field. The energy shift of each transition is calculated using Eq. (2) and the calculated reduced matrix elements for each state. The actual distribution of population among the magnetic sublevels is found by resolving the Zeeman structure of the two states, and measuring the peak amplitude of each transition. These amplitudes are used as weights in a sum of the shifts of each state due to Eq. (2) to determine the average shift of the unresolved line. The average shift in the $B \rightarrow A$ transition frequency ω_{rf} is given by

$$\frac{\delta\omega_{\text{rf}}}{2\pi} = \pm(10^{14} \text{ Hz}) \left[500 \left(C_0^{(0)} - \frac{2U_\odot}{3c^2} c_{00} \right) + 9.1 C_0^{(2)} \right], \quad (3)$$

where $U_\odot = -M_\odot G/r_{\text{lab}}$ is the Sun's gravitational potential, and ω_{rf} is defined to be positive, producing a positive (negative) shift for ^{164}Dy (^{162}Dy). This sign difference helps reject background systematics, and is determined by the sign of the energy difference between A and B . The sign of the second term depends on the relative magnetic sublevel populations.

The value of $C_0^{(0)}$ and $C_0^{(2)}$ in the laboratory frame is a function of $c_{\mu\nu}$ in the SCCEF, and the orientation and velocity of the lab. Thus any anomalous $\delta\omega_{\text{rf}}$ measured in the lab must vary in time [17]. The precise relation

between $C_0^{(0)}$ and $C_0^{(2)}$ and the SCCEF value of $c_{\mu\nu}$ can be found in the Supplemental Material [26]. The scalar c_{TT} component of $c_{\mu\nu}$ can be bounded via frame- or gravitational potential-dependent effects, as it contributes to the modulation of $C_0^{(2)}$, scaled by Earth's orbital velocity squared $\beta_\oplus^2 \approx 1 \times 10^{-8}$, and to that of the larger scalar term in Eq. (3) via modulations of the laboratory in the Sun's gravitational potential, which have amplitude $\Delta U_\odot/c^2 = 1.7 \times 10^{-10}$.

Using repeated measurements of $\delta\omega_{\text{rf}}$ acquired over nearly two years, we obtain constraints on eight of the nine elements of $c_{\mu\nu}$. The c_{JK} coefficients are constrained using data collected over the course of 12 h beginning on Oct. 19, 2012. For each isotope the mean value of 20 successive frequency measurements (~ 10 sec) is assigned an error bar according to the standard error of the mean for that bin. The resulting data are fit to Eq. (3) in terms of c_{JK} in the SCCEF [26], augmented by an independent, constant frequency offset for each isotope. The short duration of this data set allows us to neglect the slow (1 and 2 yr^{-1}) variations induced by the c_{TT} and c_{TJ} terms. These terms are neglected in this fit, as they are suppressed by at least one factor of $\beta_\oplus \sim 10^{-4}$, and existing limits [14] on these terms constrains their contributions well below our statistical sensitivity.

The c_{TJ} and c_{TT} coefficients are constrained using data collected between November 2010 and July 2012. The data are binned and assigned error bars as previously described. Since the above analysis of the 12 h data set provides tight constraints on c_{JK} coefficients, the second fit includes only the c_{TJ} and c_{TT} coefficients. The fit routine is the same as before, adding an independent linear slope for each isotope to account for long-term systematic drifts. The resulting fit includes a large signal for the combination $c_{T(Y-Z)} \equiv c_{TY} \sin\eta - c_{TZ} \cos\eta = (-21 \pm 2.2) \times 10^{-13}$, where η is the Earth's axial tilt. As such a signal is inconsistent with existing limits on $c_{T(Y-Z)}$ [13,14], we suspect the presence of uncontrolled systematic shifts in $\delta\omega_{\text{rf}}$ with characteristic modulation frequencies near 1 and 2 day^{-1} , and amplitude 300 mHz. These systematics may be due in part to, e.g., magnetic field fluctuations (~ 50 mHz), blackbody shifts due to changes in the temperature of the spectroscopy chamber (~ 60 mHz) [31], and changes in electronic offsets (~ 140 mHz). Daily fluctuations in these systematic shifts have less effect on our bounds on c_{TX} and $c_{T(Y+Z)} \equiv c_{TY} \cos\eta + c_{TZ} \sin\eta$, as these are primarily sensitive to the yearly modulation signal produced by the larger scalar component of Eq. (3) [26]. In the presence of correlated noise, our statistical error bars overstate our measurement's precision; thus, we repeat the least-squares analysis without flipping signs for ^{162}Dy relative to ^{164}Dy . This model is insensitive to Lorentz violation, but is sensitive to systematic error. Where they are larger, the absolute mean of each term in this fit replaces the statistical error estimated by the original fit.

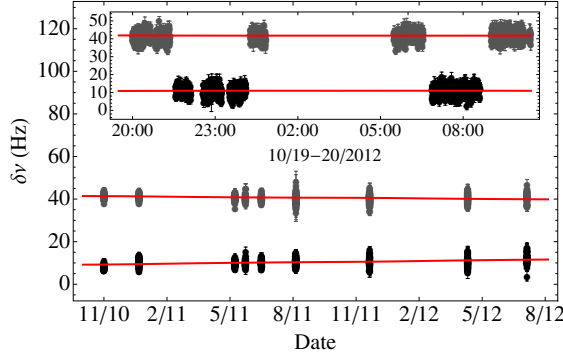


FIG. 2 (color online). Full record of frequency measurements for ^{162}Dy (upper data set) and ^{164}Dy (lower data set). Frequencies are plotted relative to 234 661 065 Hz for ^{162}Dy and 753 513 695 Hz for ^{164}Dy . Error bars are obtained by binning measurements into sets of 20 and calculating the standard error of the mean for each set. The solid line indicates the least-squares fit. Inset: an expanded view of the most recent measurements beginning on Oct. 19, 2012, with time given in Pacific Standard Time (Coordinated Universal Time minus 8 hours).

We have also analyzed our results as a test of the gravitational redshift for electrons in the Sun's gravitational potential by fitting the long term data to terms proportional to the gravitational potential, neglecting frame-dependent effects. We obtain a purely gravitational limit on the electron's c_{TT} coefficient of $-14 \pm 28 \times 10^{-9}$.

The data and fits are shown in Fig. 2. The fit results are displayed in Table II with uncertainties quoted for 68% confidence limits. The reduced chi-squared, $\bar{\chi}^2$, for the short and long time scale fits are 1.2 and 1.8, respectively.

TABLE II. Constraints on electron $c_{\mu\nu}$ -coefficients from spectroscopy of the rf transitions in ^{162}Dy and ^{164}Dy . We use the shorthand notation $c_{X-Y} \equiv c_{XX} - c_{YY}$, $c_{T(Y+Z)} \equiv c_{TY} \cos \eta + c_{TZ} \sin \eta$, and $c_{T(Y-Z)} \equiv c_{TY} \sin \eta - c_{TZ} \cos \eta$, where $\eta = 23.4^\circ$ is the angle between the Earth's spin and orbital axes. Bounds above the horizontal divider are obtained from 12 h of continuous measurement, while those below the line are obtained from analysis of over 2 yr of data, see text. Some uncertainties for the latter limits are adjusted for systematic error; the statistical uncertainty is then indicated in parenthesis. Past bounds on c_{JK} , c_{TJ} , and c_{TT} , and the purely gravitational limit on c_{TT} are from analyses reported in [12–14,16], respectively.

| Combination | New limit | Existing limit |
|-------------------------------|--------------------|-----------------------------------|
| $0.10c_{X-Y} - 0.99c_{XZ}$ | -9.0 ± 11 | $27 \pm 19 \times 10^{-17}$ |
| $0.99c_{X-Y} + 0.10c_{XZ}$ | 3.8 ± 5.6 | $-32 \pm 62 \times 10^{-17}$ |
| $0.94c_{XY} - 0.35c_{YZ}$ | -0.4 ± 2.8 | $43 \pm 19 \times 10^{-17}$ |
| $0.35c_{XY} + 0.94c_{YZ}$ | 3.2 ± 7.0 | $5.3 \pm 23 \times 10^{-17}$ |
| $0.18c_{TX} - 0.98c_{T(Y+Z)}$ | $0.95 \pm 18(3.3)$ | $-0.7 \pm 1.3 \times 10^{-15}$ |
| $0.98c_{TX} + 0.18c_{T(Y+Z)}$ | $5.6 \pm 7.7(2.4)$ | $-1.4 \pm 5.4 \times 10^{-15}$ |
| $c_{T(Y-Z)}$ | $-21 \pm 19(2.2)$ | $.002 \pm .004 \times 10^{-13}$ |
| c_{TT} | $-8.8 \pm 5.1(4)$ | $10^{-6}(2 \pm 2) \times 10^{-9}$ |
| c_{TT} (gravitational) | $-14 \pm 28(9)$ | $4600 \pm 4600 \times 10^{-9}$ |

The larger $\bar{\chi}^2$ of the long-term fit is likely due to uncontrolled systematics that have not been accounted for in our purely statistical estimation of error bars. To obtain conservative estimates on parameter uncertainties we have scaled the statistical error bars in both fits to provide $\bar{\chi}^2 = 1$. For the parameters bounded by the long-term fit, even the rescaled statistical limits are smaller than our estimated systematic errors, and so we conservatively conclude that these Lorentz-violating coefficients are at least no larger than our estimated systematic error.

We have tightened experimental limits on four of the six parity-even components of the $c_{\mu\nu}$ tensor by factors ranging from 2 to 10 [4,12]. We report limits on two combinations of the parity-odd c_{TJ} that are on par with those set by ~ 50 TeV astrophysical phenomena [4,14]. We improve bounds on electron-related anomalies in the gravitational redshift by a factor of 160, to 2.8×10^{-8} . With optimization, our experiment could yield significantly improved constraints. As Fig. 3 shows, our experiment is statistically sensitive to $C_0^{(2)} = c_{jj} - 3c_{33}$ in the lab at the level of 2.2×10^{-16} after 400 sec of averaging. At present, we must wait a full day for the Earth to rotate the laboratory in the fixed reference frame, increasing our susceptibility to systematics varying on that time scale. This could be addressed by active rotation of the entire apparatus, or of the polarization of the rf electric field, making possible statistically limited sensitivities to $C_0^{(2)}$ at the level of 1.5×10^{-17} in one day, and 7.8×10^{-19} in a year. Optically pumping the atoms to the $M = \pm 10$ states could increase the experiment's sensitivity to $C_0^{(2)}$ by a factor of ~ 4.5 . Increasing the interaction time of the atoms in the rf field could gain another factor of two, as the measured linewidth of 40 kHz is twice the natural linewidth of state A. An optimized experiment may thus reach sensitivities at the order of 8.7×10^{-20} in one year. This would be 3 orders of magnitude better than the presently reported limits on c_{JK} , 2 orders of magnitude better than the best sensitivities attainable by existing optical resonator tests [32], and could prove more sensitive than astrophysical tests [14,33]. Still narrower linewidths are possible in spectroscopic measurements of the Zeeman and hyperfine structure of the ground state of trapped Dy [34], other

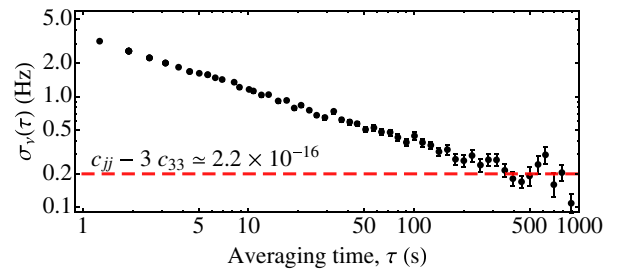


FIG. 3 (color online). Allan deviation from a two hour measurement of the ^{164}Dy transition frequency (7:00 to 9:00 on the Fig. 2 inset).

rare-earth elements, and of the long-lived states of rare-earth ions in doped materials. Optical transition energies in trapped ion or neutral atom clocks, and of the electronic and rovibrational states of molecules may also be sensitive to $c_{\mu\nu}$. The latter might also probe violations of LLI and EEP for nuclei. The derivation of the scalar and quadrupole moments of the involved states will be the subject of future work.

We are grateful to Andreas Gerhardus, Paul Hamilton, Alan Kostelecký, Jay Tasson, and Christian Weber for stimulating discussions. D.B. acknowledges support from the Miller Institute for Basic Research in Science. We are grateful to Arman Cingöz, Valeriy Yashchuk, Alaine Lapierre, and Tuan Nguyen for designing and building the Dy atomic-beam machine. We thank Holger Müller for support of this work. This work is supported by the Australian Research Council, the National Science Foundation, and the Foundational Questions Institute.

*hohensee@berkeley.edu

- [1] C. W. Misner, K. S. Thorne, and J. A. Wheeler, *Gravitation* (Freeman, San Francisco, 1970).
- [2] V. A. Kostelecký and S. Samuel, *Phys. Rev. D* **39**, 683 (1989).
- [3] T. Damour, *Classical Quantum Gravity* **13**, A33 (1996).
- [4] V. A. Kostelecký and N. Russell, *Rev. Mod. Phys.* **83**, 11 (2011).
- [5] C. M. Will, *Living Rev. Relativity* **9**, 3 (2006).
- [6] D. Colladay and V. A. Kostelecký, *Phys. Rev. D* **55**, 6760 (1997); **58**, 116002 (1998); V. A. Kostelecký, *Phys. Rev. D* **69**, 105009 (2004).
- [7] V. A. Kostelecký and J. D. Tasson, *Phys. Rev. D* **83**, 016013 (2011).
- [8] V. A. Dzuba, V. V. Flambaum, and I. B. Khriplovich, *Z. Phys. D* **1**, 243 (1986).
- [9] V. A. Dzuba, V. V. Flambaum, and J. K. Webb, *Phys. Rev. Lett.* **82**, 888 (1999); *Phys. Rev. A* **59**, 230 (1999).
- [10] V. A. Dzuba, V. V. Flambaum, and M. G. Kozlov, *Phys. Rev. A* **50**, 3812 (1994).
- [11] V. A. Dzuba, V. V. Flambaum, and M. V. Marchenko, *Phys. Rev. A* **68**, 022506 (2003).
- [12] H. Müller, P. Stanwix, M. Tobar, E. Ivanov, P. Wolf, S. Herrmann, A. Senger, E. Kovalchuk, and A. Peters, *Phys. Rev. Lett.* **99**, 050401 (2007).
- [13] B. Altschul, *Phys. Rev. D* **82**, 016002 (2010).
- [14] B. Altschul, *Phys. Rev. Lett.* **96**, 201101 (2006); *Phys. Rev. D* **74**, 083003 (2006).
- [15] R. F. C. Vessot *et al.*, *Phys. Rev. Lett.* **45**, 2081 (1980).
- [16] M. A. Hohensee, S. Chu, A. Peters, and H. Müller, *Phys. Rev. Lett.* **106**, 151102 (2011).
- [17] V. A. Kostelecký and C. D. Lane, *Phys. Rev. D* **60**, 116010 (1999).
- [18] R. Bluhm, V. A. Kostelecký, C. D. Lane, and N. Russell, *Phys. Rev. Lett.* **88**, 090801 (2002); *Phys. Rev. D* **68**, 125008 (2003).
- [19] B. Altschul, *Phys. Rev. D* **81**, 041701 (2010).
- [20] V. A. Kostelecký and C. D. Lane, *J. Math. Phys. (N.Y.)* **40**, 6245 (1999).
- [21] M. A. Hohensee and H. Müller (to be published).
- [22] V. A. Dzuba and V. V. Flambaum, *Phys. Rev. A* **77**, 012514 (2008); *Phys. Rev. A* **77**, 012515 (2008).
- [23] V. A. Dzuba, *Phys. Rev. A* **71**, 032512 (2005); V. A. Dzuba and V. V. Flambaum, *Phys. Rev. A* **75**, 052504 (2007).
- [24] W. C. Martin, R. Zalubas, and L. Hagan, *Atomic Energy Levels—The Rare-Earth Elements* (NIST, Washington, 1978).
- [25] V. A. Dzuba and V. V. Flambaum, *Phys. Rev. A* **81**, 052515 (2010).
- [26] See Supplemental Material at <http://link.aps.org/supplemental/10.1103/PhysRevLett.111.050401> for the derivation of the matrix elements of the states A and B , and the expression for Eq. (3) in terms of $c_{\mu\nu}$ in the SCCEF.
- [27] A. T. Nguyen and D. Budker, S. K. Lamoreaux, and J. R. Torgerson, *Phys. Rev. A* **69**, 022105 (2004).
- [28] A. Cingöz, A. Lapierre, A.-T. Nguyen, N. Leefler, D. Budker, S. K. Lamoreaux, and J. R. Torgerson, *Phys. Rev. Lett.* **98**, 040801 (2007); S. J. Ferrell, A. Cingöz, A. Lapierre, A.-T. Nguyen, N. Leefler, D. Budker, V. V. Flambaum, S. K. Lamoreaux, and J. R. Torgerson, *Phys. Rev. A* **76**, 062104 (2007).
- [29] N. Leefler, C. T. M. Weber, A. Cingöz, J. R. Torgerson, and D. Budker, [arXiv:1304.6940](https://arxiv.org/abs/1304.6940).
- [30] N. Leefler, A. Cingöz, D. Budker, S. J. Ferrell, V. V. Yashchuk, A. Lapierre, A.-T. Nguyen, S. K. Lamoreaux, and J. R. Torgerson, in *Proceedings of the 7th Symposium Frequency Standards and Metrology, Asilomar, October 2008*, edited by L. Maleki (World Scientific, Singapore, 2009), p. 34.
- [31] C. T. M. Weber *et al.* (to be published).
- [32] S. Herrmann, A. Senger, K. Möhle, M. Nagel, E. V. Kovalchuk, and A. Peters, *Phys. Rev. D* **80**, 105011 (2009); Ch. Eisele, A. Yu. Nevsky, and S. Schiller, *Phys. Rev. Lett.* **103**, 090401 (2009).
- [33] F. R. Klinkhamer and M. Schreck, *Phys. Rev. D* **78**, 085026 (2008).
- [34] M. Lu, S. H. Youn, and B. L. Lev, *Phys. Rev. Lett.* **104**, 063001 (2010).